Surface Segregation of Counterions in Ionomer Films

Russel M. Walters,[†,‡] Andreas Taubert,[§,||] Joon-Seop Kim,[⊥] Karen I. Winey,[*,§] and Russell J. Composto[*,§]

Department of Chemical and Biomolecular Engineering, University of Pennsylvania, Philadelphia, Pennsylvania 19104, Department of Materials Science and Engineering, University of Pennsylvania, Philadelphia, Pennsylvania 19104-6272, and Polymer Science Department, Chosun University, Gwangju, Korea

Received August 1, 2008; Revised Manuscript Received October 9, 2008

ABSTRACT: The surface segregation of cations in a poly(styrene-*ran*-methacrylic acid) ionomer fully neutralized with Cs was demonstrated using Rutherford backscattering spectrometry (RBS), scanning force microscopy (SFM), and scanning transmission electron microscopy (STEM). Whereas spin-cast films and those annealed below ∼120 °C exhibit a uniform distribution of Cs, a surface excess of Cs was observed for films annealed at higher temperatures. At long times (>30 h) and high temperatures (>145 °C), the surface concentration of Cs approached a constant value of two-thirds of the total Cs in the film. Although Cs-rich vesicular aggregates (∼8−85 nm diameter) were observed in all films, the surface excess of Cs coincided with nanometer-sized features on the surface. Based on these results, a mechanism was proposed that accounts for cation mobility and a driving force for surface segregation. At elevated temperatures, Cs ions initially in cation-acid lone pairs are solubilized by favorable cation-π interactions facilitated by styrene monomers. Above ∼120 °C, these solubilized cations are sufficiently mobile to diffuse. The driving force to the surface arises from the concentration gradient established when Cs at the surface scavenges Cl from the environment to form CsCl. In the polystyrene-based ionomers, surface segregation is not observed if either the cation mobility is reduced by using a divalent cation or the driving force for surface segregation is removed by eliminating atmospheric Cl.

Introduction

Ionomers are neutralized acid-containing copolymers having a majority of hydrophobic monomers and a minority of monomers (<15%) containing acid groups.[1] The acid groups and counterions form complexes that can persist as cation−acid lone pairs or can microphase separate from the hydrophobic majority phase to form nanoscale ionic aggregates. A unique characteristic of ionomers is that these ionic aggregates act as cross-links that impart favorable bulk properties such as toughness and environmental stability. The surface properties, which are of particular interest here, make ionomers excellent packaging materials, because their oil and grease resistance allows them to seal complex products such as meats.[2]

Although ionomers were first commercialized in the 1960s, the numerous chemical and processing variables that influence ionomer morphology and properties have hindered the development of a thorough understanding. In particular, ionomer structures and properties depend on the acid content of the copolymer, the acid type, the fraction of acid groups neutralized by counterions, the counterion type, and the hydrophobic monomer type. Advanced understanding of ionomer structure,[3] transport[4−6] and surface properties is now evolving with the application of powerful new techniques for depth profiling, dielectric spectroscopy,[7,8] electron spin resonance,[9] and imaging.[10−13] Furthermore, the strong specific interactions between the ionic groups in these materials virtually guarantee that equilibrium structures cannot be produced. This accentuates the importance of specimen preparation and handling, which we have recently explored.[14−16]

A series of morphological studies have recently been completed using X-ray scattering, high angle annular dark field scanning transmission electron microscopy (HAADF STEM), and image simulation.[12,13] The ionomer under investigation was prepared by solution neutralizing a poly(styrene-ran-methacrylic acid) (SMAA) random copolymer using copper acetate, recovering the fully neutralized ionomer via solvent casting, drying and annealing. The morphology consisted of monodisperse, spherical ionic aggregates (∼1.0 nm diameter) uniformly distributed in the ionomer. When this same ionomer was recovered via precipitation, the Cu-rich domains varied widely in size (∼5−50 nm diameters), but annealing above the glass transition temperature transformed this ionomer into the morphology produced by solvent casting.[15] In contrast, a study of SMAA fully neutralized with Cs and isolated by freeze-drying uncovered vesicular aggregates with diameters ranging from 5−45 nm and shell thicknesses of ∼3 nm.[17] These morphological studies demonstrate that processing methods can alter the spatial distribution of cations in ionomers.

Recent studies have begun to examine the surface characteristics of ionomer films. In Nafion, normal tapping mode scanning force microscopy (SFM) was used to image crystallites, whereas low oscillation amplitude SFM was used to resolve the ionic domains near the surface.[18] Interpreting height and phase images, the near-surface morphology was found to contain ∼10 nm crystallites and ionic domains coated by a thin, F-rich surface layer (<1 nm). No ionic species were found at the outermost few angstroms of the surface, but rather ionic domains were detected a few nanometers below the surface. To account for the observed rapid diffusion of water into Nafion, McLean et al. proposed that ionic domains quickly diffuse to the surface upon exposure to water. This rearrangement was attributed to the repulsion and attraction of the hydrophobic surface layer and ionic species, respectively.

* Corresponding authors. E-mail: (R.J.C.) composto@seas.upenn.edu; (K.I.W.) winey@seas.upenn.edu.
[†] Department of Chemical and Biomolecular Engineering, University of Pennsylvania.
[‡] Current address: Johnson & Johnson, Skillman, New Jersey 08558.
[§] Department of Materials Science and Engineering, University of Pennsylvania.
[||] Current address: Institute of Chemistry, University of Potsdam, Potsdam, Germany.
[⊥] Polymer Science Department, Chosun University.

10.1021/ma801756g CCC: $40.75
Published on Web 11/07/2008

In subsequent studies,[19] these SFM methods were used to image crystal and ionic domains in poly(ethylene-*ran*-methacrylic acid) (EMAA) partially neutralized by Na and Zn. The ethylene lamellar dimensions from SFM were found to be in reasonable agreement with bulk samples characterized by SAXS. Using low oscillation amplitude SFM, the ionic domains below the surface were found to be ~10−15 nm wide but several tens of nanometers long. This suggests that the method detects overlapping ionic domains. It is interesting that water contact angles were consistent with a surface composition similar to pure polyethylene. Namely, the outermost surface is apparently covered by ~1 nm of amorphous hydrocarbon. These samples were melt pressed against a smooth hydrophobic surface at 180 °C for an unspecified time and allowed to cool to room temperature. The effects of processing conditions on surface morphology were not investigated, so it is difficult to generalize these results.

In this paper, a systematic study of the surface composition of a poly(styrene-*ran*-methacrylic acid) ionomer fully neutralized by Cs is performed using Rutherford backscattering spectrometry. Three segregation regimes are observed for Cs counterions corresponding to no segregation observed at low annealing temperatures and all times, incomplete or kinetically limited segregation at intermediate temperatures and times, and complete segregation at high temperatures and long times. Complimentary scanning transmission electron microscopy (STEM) and SFM studies show that surface segregation coincides with the persistence of vesicular aggregates and the formation and coarsening of surface features. A mechanism for cation surface segregation is proposed that accounts for both cation mobility and the driving force for cation surface enrichment.

Experimental Methods

Materials. Poly(styrene-*ran*-methacrylic acid) (SMAA) was prepared by free radical copolymerization and has 6.1 mol % methacrylic acid. This copolymer was dissolved in benzene/methanol (9/1 v/v) and fully neutralized by a solution of cesium hydroxide (CsOH) in methanol. The solution was stirred for 30 min and then freeze-dried.

To prepare samples for Rutherford backscattering spectrometry (RBS) and scanning force microscopy (SFM), the Cs−SMAA was dissolved in toluene/methanol (9/1 v/v), and spun cast at 2000 rpm onto 2 × 2 cm silicon wafers that were cleaned with HF. These films were dried at 80 °C overnight and have a thickness of ~ 400 nm, as measured by ellipsometry. Samples were annealed (90 to 210 °C) at pressures of $\sim 10^{-2}$ Torr for up to 100 h. Samples were also prepared by a solvent-free method, where the freeze-dried powder of Cs−SMAA was compression molded (9000 N, 150 °C, 20 min). These melt pressed samples have a thickness of ~0.5 mm and were annealed under vacuum (175 °C, 1 week).

For scanning transmission electron microscopy (STEM) experiments thinner, electron-transparent samples were prepared. By reducing the concentration of the polymer solution, thinner films (75 nm by ellipsometry) were spun cast and then floated off the wafer onto deionized water and collected onto carbon-coated copper TEM grids. The films on TEM grids were annealed in vacuum oven and stored under vacuum at room temperature.

Techniques. Rutherford backscattering spectrometry (RBS) is an excellent tool for tracking high atomic number (Z) elements and was used to determine the Cs concentration as a function of depth in Cs−SMAA films. Elemental resolution is achieved in RBS by backscattering a light projectile, He^+, from heavier elements in the sample. Because Cs ($Z = 55$) has a much higher Z than the other elements in the film (H ($Z = 1$), C ($Z = 6$), and O ($Z = 8$)), Cs is readily resolved. Using 2.000 MeV He^+, the depth resolution was enhanced by choosing a grazing incidence geometry with incident and scattering angles of $\alpha = 15°$ and $\theta = 10°$, respectively. For each sample, 10 μC of charge was collected at a beam current of 10 nA. Raw RBS spectra in yield versus energy are converted to concentration versus depth as follows. The energy of the backscattered helium ion was converted to depth in the sample using the slab approach.[20] The yield of helium ions was converted to atomic concentration (cf., Figures 1 and 3) by dividing the measured yield by values from a known standard. Simulations were performed using the program RUMP.[21] Fixing experimental conditions (e.g., geometry and beam energy), simulations were fit to the experimental data by varying the Cs depth profile (cf., Figure 2).[20]

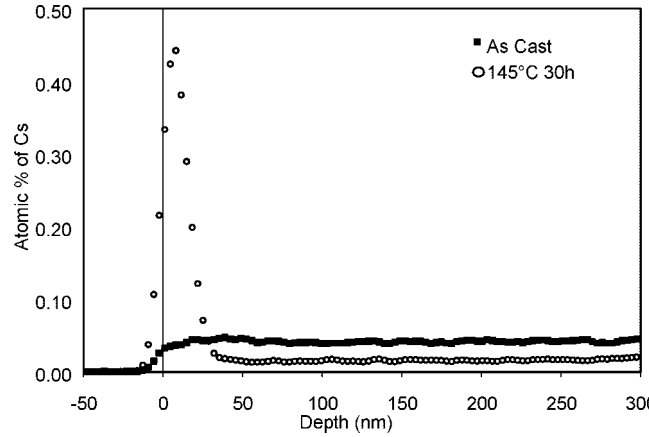

Figure 1. Converted Rutherford backscattering spectrometry (RBS) data from an unannealed, spun-cast film (■) of Cs−SMAA with a uniform concentration of the Cs counterion throughout the film, and a film annealed at 145 °C for 30 h (○) displaying surface segregation of the Cs counterion. A depth of zero represents the free surface and is determined by deconvoluting the instrumental resolution from the experimental profile. The films are ~400 nm thick.

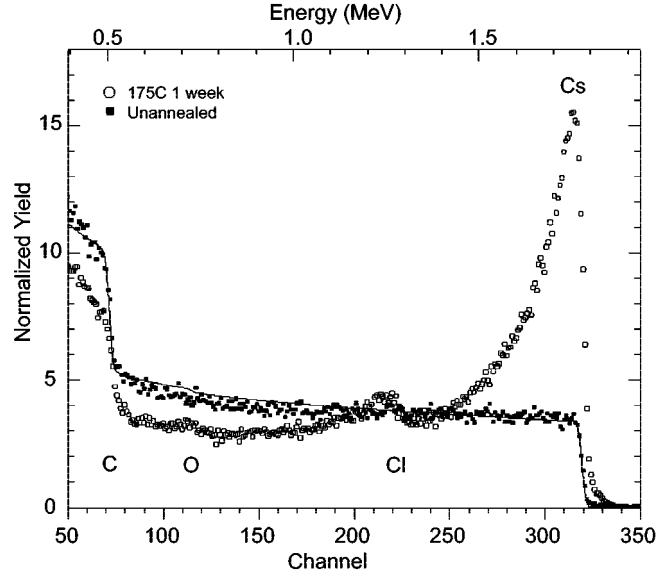

Figure 2. RBS spectra from compression molded Cs−SMAA ionomers: (■) unannealed sample and (○) sample after 1 week at 175 °C. The unannealed sample has a uniform distribution of Cs, whereas the annealed sample shows Cs and Cl segregation at the air interface. In the RBS spectra the surface energies (channels) of Cs, Cl, O, and C are identified in the figure.

The Cs surface excess was calculated by determining the surface concentration (i.e., area under the peak) and then subtracting the background due to the bulk concentration of Cs. The back edge of the Cs surface peak was defined at a depth at which the Cs concentration reached the bulk concentration. The surface topography of the samples was imaged by scanning force microscopy (SFM) in tapping mode using a Digital Instrument Multimode (scan sizes 1.5 μm × 1.5 μm, scan rate 1 Hz).

Scanning transmission electron microscopy was performed on a JEOL 2010F FEG S/TEM, as described previously.[17] Images were

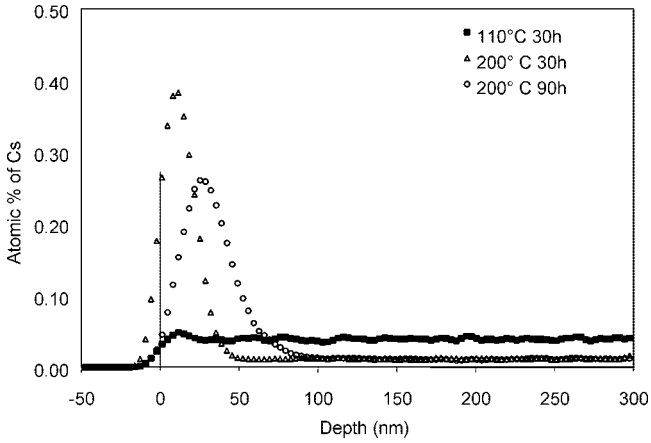

Figure 3. Depth profile of Cs in Cs−SMAA films after annealing at 200 °C for 30 h (Δ) and 90 h (○). After annealing at 110 °C for 30 h (■), surface segregation is not observed. The small peak results from segregation during solvent evaporation.

collected with a high angle annular dark field (HAADF) detector that accentuates the atomic number differences and reduces the contribution from phase contrast. In projection, Cs-rich features appear bright in the images.

Results and Discussion

Surface Segregation by RBS. Figure 1 shows the atomic percent of Cs as a function of depth in as-cast and annealed Cs−SMAA films. In the as-cast film, Cs is uniformly distributed throughout the film and, furthermore, the bulk Cs composition measured by RBS is in excellent agreement with the 0.39 at. % calculated for a fully neutralized SMAA with 6.1 mol % acid groups. Upon annealing, the Cs depth profile is no longer uniform and exhibits a surface excess at the free surface. Correspondingly, the Cs concentration in the bulk (away from the surface of the film) has decreased relative to the as-cast film. By integrating the surface excess peak, we found that 58% of the Cs in the film segregates to the surface upon annealing at 145 °C for 30 h, while the other 42% remains in the bulk of the film.

From the known ionomer composition, the Cs:C atomic ratio is 1:127, corresponding to 1 Cs for every 16 monomeric units or 1 Cs for each acid group. The resulting SMAA stoichiometry is $C_8H_{8.1}O_{0.12}Cs_{0.63}$. This composition is used to simulate RBS spectra and the agreement is excellent in Cs−SMAA films without surface segregations. In contrast, the surface excess of Cs observed in Figure 1 is accurately simulated by a 20 nm Cs-rich surface layer that contains a Cs:C ratio of 1:4. This Cs:C ratio would allow for a surface layer consisting of only Cs and acid monomers. However, such an arrangement is physically unlikely because the acid groups are randomly distributed along the copolymer, and therefore it is improbable that Cs-neutralized acid groups can form a 20 nm thick surface layer. This analysis suggests that the majority of the surface segregated Cs atoms are dissociated from the acid groups.

In addition to observing surface segregation in these solvent cast films, surface segregation of Cs was also observed when a thick Cs−SMAA sample was prepared by compression molding and then annealed, Figure 2. In the RBS analysis, these samples are considered semi-infinitely thick. In the as-molded sample, the front edge of the signal at 1.8 MeV corresponds to $^{+}$He backscattering from Cs atoms at the free surface. The plateau at lower energies corresponds to backscattering from Cs atoms below the surface. Near 0.5 MeV, the carbon front edge appears and its plateau adds to the Cs plateau. The solid line is a simulation for a semi-infinite thick film having the stoichiometry, $C_8H_{8.1}O_{0.12}Cs_{0.63}$, as discussed above. In the as-molded sample, the Cs concentration is uniform over a depth on nearly 2 μm. In contrast, the annealed thick sample has a large surface excess of Cs (1.5−1.8 MeV). Because compression molded films are much rougher than the spin-cast films, the back-edge of the Cs signal shows an extensive tail making quantitative simulations difficult. Below this surface excess layer, the annealed thick sample shows a decrease in the bulk Cs concentration relative to the as-molded (0.6−1.0 MeV).

The RBS spectrum of the annealed thick sample also contains a prominent feature with a front edge at 1.26 MeV that corresponds to a surface excess of Cl, Figure 2. Note that the shape of the Cl signal mimics that of the Cs profile. The Cl signal is weaker because its cross-section, which scales as Z^2, is much lower than Cs. RBS analysis of the two surface layers on this thick sample reveals a Cs:Cl ratio of $\sim$ 1:1. This stoichiometry suggests that the Cl neutralizes Cs ions to form CsCl at the surface. For the unannealed, as-molded thick ionomer, no Cl signal in the RBS spectrum is observed. In summary, the thermally induced surface segregation of Cs in spun-cast ionomer films is also observed in macroscopic (compression molded) samples where the Cs segregation is also accompanied by surface enrichment of Cl.

The remainder of this section discusses control studies aimed at understanding the origin of Cl. The Supporting Information presents a comprehensive study of Cl investigated by RBS for various stages of Cs surface segregation. To summarize these findings, Cl is not observed in any Cs−SMAA film that displays a uniform Cs concentration (no segregation). However in samples that exhibit Cs surface segregation, the peak area (concentration) and peak shape (position) of the Cl signal correlates with that of the Cs signal. Thus, the amount and position of the Cl at the surface correlates with Cs and the observed Cs:Cl ratio is $\sim$1:1.

In agreement with the RBS studies, elemental analysis did not detect any Cl in nonannealed Cs−SMAA. These experiments were conducted by Galbraith Laboratories Inc. (Knoxville, TN) and the detection limit was 300 ppm. If the surface excess of Cl originated only from the starting material, the Cl content would have to be $\sim$3500 ppm, much greater than the detection limit. Furthermore, X-ray energy dispersive spectroscopy (XEDS) analysis of as-cast films did not detect Cl, although Cl was readily detected after annealing. In summary, in the as prepared Cs−SMAA ionomer films, Cl does not exist at concentrations that would account for the measured surface excess.

We attribute the Cl found in the annealed samples to atmospheric Cl. During annealing at temperatures from 110 to 200 °C, samples are heated in a closed chamber under "vacuum" at a moderate pressure of $\sim 10^{-2}$ Torr. Under these conditions, the samples are continually exposed to Cl, which exists in the ambient atmosphere as various species.[22−24] The concentration of Cl species is sufficient to account for the amount of Cl found in the samples contain excess Cs and Cl at the surface. This hypothesis was tested by annealing two samples that were placed side-by-side in a vacuum oven. One sample was encapsulated in a sealed evacuated glass tube and the other exposed to the atmosphere in the chamber. The encapsulated sample was prepared by inserting a sample into a glass tube ($\sim$1/400 the volume of the oven chamber), evacuating the tube to 10^{-4} Torr, and flame sealing the tube. Both samples were annealed at 200 °C for 30 h. Whereas the exposed sample exhibited Cs surface segregation, the encapsulated sample did not. These experiment demonstrate that (1) Cl is required for the surface segregation of Cs, and (2) the primary source of Cl is from the atmosphere in the annealing chamber.

Dynamics of Surface Segregation. Figure 3 shows the Cs depth profiles for Cs−SMAA films annealed over a range of temperatures and times. Note that a small surface excess is

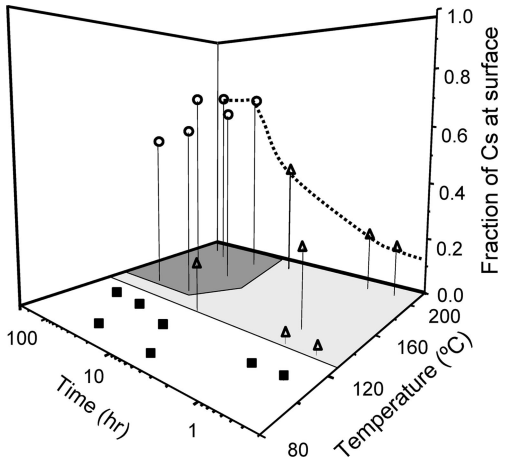

Figure 4. Fraction of Cs at the surface is shown as a function of the annealing time and temperature. Three regions are evident: (■) no surface segregation for temperatures below ~120 °C; (Δ) incomplete segregation at moderate temperatures and times where segregation is diffusion limited; (○) complete surface segregation. The dotted line shows the surface fraction of Cs as a function of time at 210 °C.

commonly observed in as-cast Cs−SMAA films (not shown) suggesting that some segregation occurs during solvent evaporation when spin coating. In Figure 3, the Cs profile after 30 h at 110 °C is comparable to that of an as-cast sample with only a slight surface excess of Cs; a similar profile was observed after annealing for only 11 h at 110 °C. In contrast, the Cs−SMAA film annealed at 200 °C for 30 h has a relative surface concentration of 67% Cs and a bulk value of 32% Cs. Films annealed at 200 °C for 90 h continued to have a relative bulk concentration of 32% Cs at depths below 100 nm. Although the surface concentration of Cs is fixed at ~68% for longer annealing times at 200 °C, the peak width increases and peak height decreases reflecting changes in surface morphology detailed below.

For Cs−SMAA films annealed at 145 °C (30 h) and 200 °C (30 and 90 h), the surface excess of Cs is ~67% and the bulk concentration is ~33% as shown in Figures 1 and 2, respectively. Thus, the Cs homogeneously distributed in the as-cast film has redistributed itself accordingly. In contrast, low annealing temperatures (e.g., 110 °C) fail to produce surface segregation as shown in Figure 3. These results suggest that surface segregation is complete after $\sim^2/_3$ of the Cs has enriched the surface and that the remaining Cs is stable in the bulk of the film.

Figure 4 shows how the extent of surface segregation or atomic fraction of Cs at the surface depends on annealing temperature and time. Three regimes are evident from Figure 4: no surface segregation (squares), incomplete surface segregation (triangles), and complete surface segregation (circles). Surface segregation was not observed at temperatures below ~120 °C for up to 100 h, suggesting that an activation temperature is required for surface segregation. Incomplete segregation is found above a temperature of ~130 °C for short annealing times. Here, the thermal energy is sufficient to dissociate the cation from the acid group, but the annealing time is not long enough to allow enough Cs to diffuse to the surface and reach 67%. In this regime, the surface excess increases monotonically with time until surface segregation is complete. The RBS depth profiles of partially segregated films display a surface enriched layer of Cs and a near surface layer depleted of Cs.[27] These depth profiles indicate that the Cs from the bulk diffuses down a concentration gradient toward the surface.[25] In a separate study of dynamics, the surface excess of Cs is found to increase as time to the 1/2 power, as expected in a diffusion controlled process, and the rate at which the surface excess increases also increases with temperature.[26]

For Cs−SMAA films annealed above 130 °C, complete surface segregation is observed at long times (>10 h) and the surface excess of Cs reaches a constant value of ~ 67%. This behavior suggests that the Cs in the as-cast films resides in two distinct local environments. Most Cs ($\sim^2/_3$) is located in an environment that allows them to dissociate from the acid groups and segregate to the surface under proper annealing conditions (Figure 4). The local environment around the remaining Cs ($\sim^1/_3$) is stable and therefore these Cs remain immobile for up to 90 h at 200 °C.

Morphology of Surface Segregation. The surface morphologies of Cs−SMAA films were characterized by SFM. The SFM images of as-cast films and films annealed below 120 °C appear featureless with only long-wavelength height variations typical of spun cast films. In contrast, surface features are apparent in partially and completely segregated Cs−MAA films. Figure 5 shows the height images and line scans for Cs−SMAA films annealed for (a) 30 h and (b) 90 h at 200 °C. Both conditions correspond to complete surface segregation. After 30 h, the film surface is covered with mounds that are ~9 nm high and nominally ~30 nm wide; this width is comparable to the lateral resolution. The number density is 180 mounds/μm^2. After 90 h, the mounds grow higher (~25 nm) and wider (~70 nm) and the number density decreases to 36 mounds/μm^{2}in Figure 5b, which suggests that the mounds can coalesce. As shown in the grazing incident RBS spectra, Figure 3, coalescence is likely responsible for the broadening of the Cs depth profile at longer times. Although their shape and number density are different, the total volume of the mounds is comparable (within 9%) for the 30 and 90 h samples. This observation agrees with the RBS results, which show that the surface excess of Cs is similar for both samples. Thus, these SFM results indicate that surface segregation of Cs is accompanied by the formation of new features on the surface and that these features coalesce with extended annealing times.

The as-cast and completely surface segregated films were also imaged using scanning transmission electron microscopy (STEM), where the images are projections of thinner films (~ 75nm) and the bright regions correspond to Cs-rich domains, Figure 6. The as-cast films have features that are consistent with vesicular ionic aggregates, Figure 6a. These ionic aggregates vary considerably in number density and size with diameters that range from 8 to 85 nm. Note that these ionic aggregates are sufficiently dilute to suggest that there are Cs−acid lone pairs dispersed in the hydrophobic matrix between the vesicular aggregates. These vesicular aggregates are similar in size and number density to the ionic aggregates observed previously in freeze-dried and compression molded samples of Cs−SMAA.[17] Upon annealing (200 °C for 30 h) to produce complete Cs surface segregation, these vesicular ionic aggregates persist with a wide variety of sizes and spatial distributions, Figure 6b. In addition, annealing produces finer scale structures in the STEM images, inset Figure 6b. These new bright features are enriched with Cs, homogeneously distributed across the sample, and uniform in size (~ 3 nm). These fine-scale Cs-rich features were not observed in the as-cast film (Figure 6a) or a film annealed at 90 °C for 30 h (no surface segregation regime; image not shown). For films annealed at 200 °C for 30 h, electron diffraction patterns from these films were indexed as CsCl with a (001) preferred orientation with respect to the surface.

Although STEM cannot discern surface from bulk features, the SFM and RBS measurements strongly suggest that the smaller scale Cs-rich structures observed in STEM are indeed on the surface. Namely, the small features that appear in the STEM and the surface mounds in SFM are attributed to surface

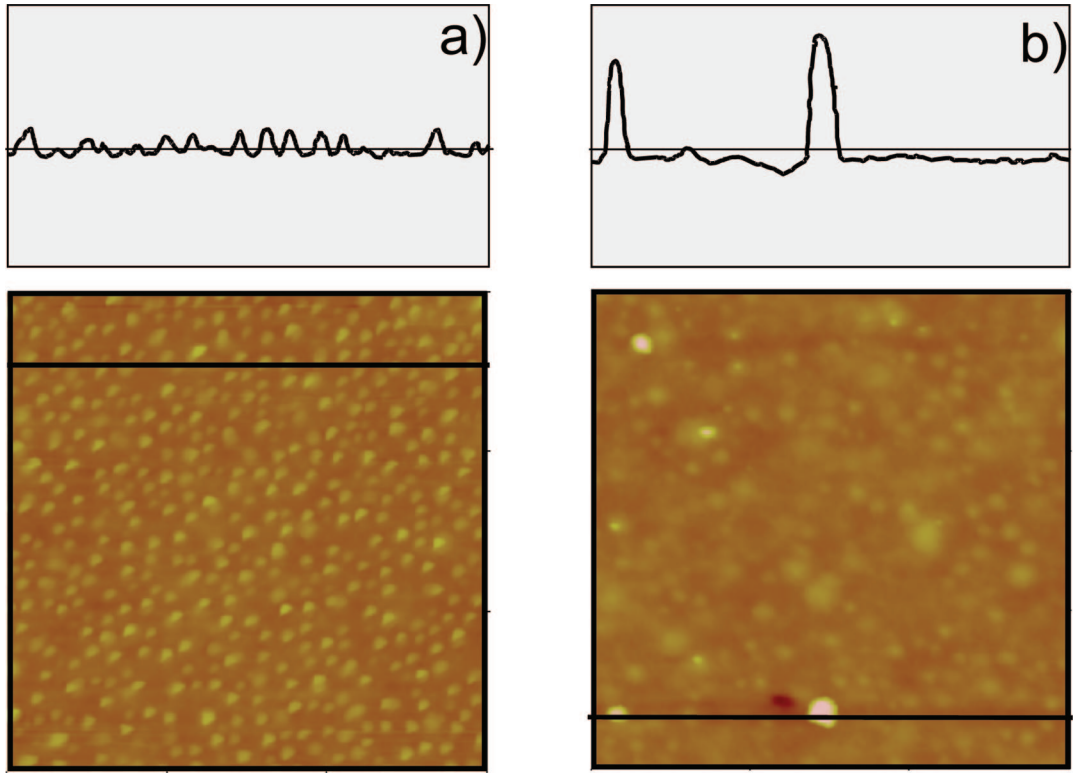

Figure 5. Scanning force microscopy (SFM) height images of a Cs−SMAA film annealed at 200 °C for (a) 30 h and (b) 90 h. Both scan sizes are 1.5 μm × 1.5 μm. Shown above each image is a line scan (1.5 μm across) corresponding to the dark line in the SFM image; the height scale is 25nm. Although the as-cast film is featureless, the surface of the film annealed for 30 h exhibits small mounds after surface segregation of the Cs counterion. Upon further annealing, for 90 h, the small mounds coalesce to form a few larger features.

segregation of Cs detected by RBS. Note that the Cs−SMAA film thickness is ∼400 nm for SFM and RBS, but is only ∼75 nm for STEM. As detailed below, this difference in film thickness accounts for the smaller quantity of surface segregated Cs and, therefore, smaller features in the STEM images (∼3 nm diameter) relative to SFM (∼30 nm) in Cs−SMAA films annealed at 200 °C for 30 h.

Surface Segregation Mechanism. Taken together, the RBS, SFM, and STEM results from Cs−SMAA films provide overwhelming evidence of Cs surface segregation and the presence of surface features. The Cs surface segregation in Cs−SMAA films requires chlorine to be present in the atmosphere and the extent of segregation depends on annealing temperature and time. The maximum surface segregation is ∼2/3 of the Cs counterions and is independent of temperature, above 130 °C. The observed surface enrichment of Cs coincides with both (1) the formation of Cs-rich surface structures that coarsen with annealing time and (2) the continued presence of Cs-rich vesicular aggregates. In the spun-cast films, the vesicular ionic aggregates are sufficiently dilute to suggest the presence of Cs−acid lone pairs dispersed in the hydrophobic matrix.

The following mechanism accounts for these combined findings. In the as-cast ionomer films, Cs is uniformly distributed through the thickness of the film. At the nanometer-scale, Cs exists either in the vesicular ionic aggregates or as cation−acid lone pairs in the SMAA matrix, Figure 7. The Cs cations in the matrix can dissociate from the carboxylic acid groups above 120 °C and thereby become mobile. The atmospheric Cl reacts with the dissociated Cs cations near the surface, which produces a concentration gradient that subsequently draws more of the dissociated Cs to the surface. In the fully segregated films, 67% of the Cs resides near the surface implying that 67% of the Cs was originally in cation-acid lone pairs in the matrix. The remaining bulk Cs (∼33%) participates in the ionic aggregates that remain intact upon annealing. Thus, for this ionomer (Cs−SMAA with 6.1 mol % acid) treated with the processing conditions in this study, the aggregation efficiency is only ∼33%.

The high fraction of Cs−acid lone pairs proposed in this mechanism is contrary to the simple assumption that all cation-acid pairs reside in ionic aggregates, but is well supported by the results. The cation-acid lone pairs might be stabilized by the styrene monomeric units, because aromatic ring interact favorably with the counterions through a cation-π interaction.[27] It has been shown that cations and aromatic rings have a strong noncovalent electrostatic attraction that involves the quadrupole moment of the aromatic ring. For example, this cation-π interaction enables benzene to compete with water in binding cations.[28] A few reports note the presence of cation-acid lone pairs in the bulk, outside of ion-rich aggregates.[29−31] Additionally, ionomer transport models[4,32] require some fraction of cation-acid lone pairs to undergo ion-hopping.

At elevated temperatures (above ∼120 °C) as the cation-acid interaction weakens, the cation-π interactions enable Cs cations to be solubilized in the hydrophobic, styrene-rich matrix. This finite solubility of Cs combined with annealing temperatures above the copolymer glass transition temperature produces mobile Cs cations. These mobile Cs cations, which are solubilized by the styrene monomeric units, can diffuse independent of the polymer chains. The mobile cations near the surface of the film scavenge Cl from the atmosphere to produce a neutral species, CsCl. This consumption of Cs produces a concentration gradient that drives more Cs toward the surface. Overall, the segregation of the Cs to the surface lowers the system free energy, because CsCl interactions are favored.

This mechanism incorporates two requirements for surface segregation: cations must have sufficient mobility to diffuse to the surface and a driving force must exist to attract these cations

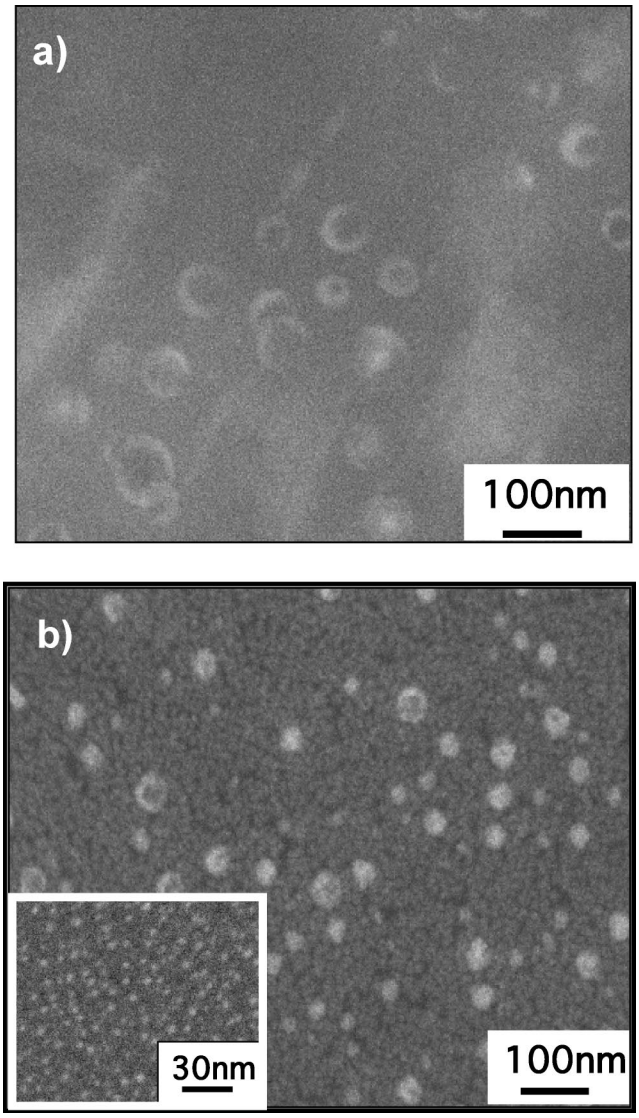

Figure 6. (a) Scanning transmission electron microscopy (STEM) image shows Cs-rich vesicular aggregates in an as-cast SMAA−Cu film. (b) After annealing at 200 °C for 30 h, conditions that have been shown to produce Cs surface segregation, the vesicle aggregates are still apparent. In addition, a small-scale structure arises that is attributed to the surface segregated Cs, inset.

to the surface. If either requirement is lacking, surface segregation does not occur. For example, when a Cs−SMAA film was annealed in a sealed vial to dramatically reduce the atmospheric chlorine, surface segregation was not observed; without Cl to scavenge Cs at the surface, a concentration gradient in Cs did not develop that would drive surface segregation. Furthermore, in SMAA films, monovalent counterions of K, Rb, and Cs were found to surface segregate, whereas the divalent counterions of Ca, Ba, Sr, and Zn did not segregate under the conditions investigated.[26] This lack of surface segregation in divalent systems indicates the absence of sufficient cation mobility due to the stronger interactions between acid groups and divalent counterions. Divalent counterions are energetically less likely to dissociate from acid groups and thus insufficiently mobile to diffuse to the surface. Both requirements, sufficient cation mobility and a driving force, are necessary for surface segregation. In these Cs−SMAA materials, mobility results from solubilizing cations via cation-π interactions at elevated temperatures and the concentration gradient of Cs is established by the formation of CsCl at the surface.

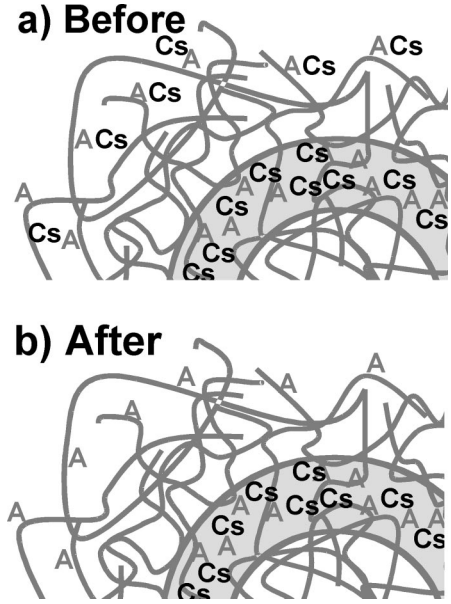

Figure 7. Schematic showing the location of Cs counterions corresponding to the proposed mechanism of surface segregation. (a) Before surface segregation, Cs counterions are located in either vesicular ionic aggregates or the bulk as cation-acid lone pairs. This morphology persists for films annealed at temperatures below ~ 120 °C. (b) During surface segregation, the Cs ions in the cation-acid lone pairs dissociate from the acid groups and diffuse to the surface. However, the Cs cations in the vesicular aggregate are stable and remain in the aggregate even at elevated temperatures.

The results in two earlier publications suggest the presence of counterion surface segregation. Handlin et al.[33] used electron microscopy methods in an attempt to image aggregates in EMAA, sulfonated polystyrene (SPS), polypentenamer, and sulfonated EPDM rubber ionomers neutralized with either K or Cs. In both solvent cast and microtomed samples, no aggregates were observed in TEM. However upon exposure to chloroform vapor, 6−10 nm features appeared randomly distributed across the sample. These features were attributed to metal salts with Cl. Based on the size and areal density of the features, the authors determined that the total amount of counterion imaged as metal salts could be supplied by the ionomer material. Colby et al.[4] measured the interdiffusion of the counterions in films of Na−SPS into Rb−SPS. To model the diffusion they applied a modified sticky reptation model. However the rate of diffusion of the counterions was observed to be 2.8×10^{-14} cm^2/s and 3.9×10^{-14} cm^2/s at 135 °C for Na and Rb, respectively, over an order of magnitude faster than their model predicted. Additionally, inspection of their counterion depth profiles suggests possible counterion surface segregation.

The counterion concentration and location in ionomers is critical for materials performance, because counterions are at the root of the enhanced physical properties. This study has shown that processing and storage conditions (temperature and time) determine the extent of surface segregation and care must be exercised to maintain a chemically homogeneous material. Counterion surface segregation will decrease the bulk counterion and thereby alter the bulk material properties, such as toughness. Furthermore, counterion surface segregation will dramatically alter the surface properties, such as wetting.

Conclusions

At high temperatures (above ~120 °C) a fraction of Cs counterions in Cs−SMAA ionomer films segregate to the air/polymer interface. This segregation has been observed in both

spun-cast and melt pressed samples when atmospheric Cl is present. In the spun-cast films, the surface segregation process reaches completion with $\sim^2/_3$ of the Cs segregated to the surface and $\sim^1/_3$ of the Cs remaining stable in the bulk. This surface segregation is accompanied by the formation of CsCl mounds that coarsen with annealing. In addition, Cs-rich ionic aggregates are present in the film and persist throughout the surface segregation progress. We propose a mechanism in which Cs−acid lone pairs exist in the as-cast and as-molded samples and these lone pairs dissociate at elevated temperatures. Dissociated cations are stabilized by cation−π interactions and exhibit considerable mobility. The dissociated cations near the surface scavenge Cl from the environment and the resulting concentration gradient in Cs drives other dissociated cations to the surface. This surface segregation ends when the cations from the cation−acid lone pairs ($\sim^2/_3$) have been consumed at the surface and only the cations in the ionic aggregates ($\sim^1/_3$) persist in the matrix. Alternative ionomers and specimen preparation methods would likely alter the proportions of cations in lone pairs and ionic aggregates, so as to control the fraction of cations that are available for surface segregation.

Acknowledgment. This research was funded by the National Science Foundation through Polymer Program Grants DMR05-49116 (K.I.W.) and DMR05-49307 (R.J.C.). Support was also provided by the MRSEC (DMR05-20020) and NSEC (DMR04-25780) programs for facility use, as well as the donors of the Petroleum Research Fund, administered by the American Chemical Society (43616-AC7) (R.J.C). We gratefully acknowledge valuable discussions with Dr. B. P. Kirkmeyer.

Supporting Information Available: Text discussing the RBS analysis of the Cs and Cl concentration as a function of the annealing temperature and time and a figure plotting the data. This material is available free of charge via the Internet at http://pubs.acs.org.

References and Notes

(1) Eisenberg, A.; Kim, J. S. *Introduction to Ionomers*; Wiley-Interscience: New York, 1998.
(2) Van Alsten, J. G. *Macromolecules* **1996**, *29*, 2163–2168.
(3) Kolbet, K. A.; Schweizer, K. S. *Macromolecules* **2000**, *33*, 1425–1442.
(4) Colby, R. H.; Zheng, X.; Rafailovich, M. H.; Sokolov, J.; Peiffer, D. G.; Schwarz, S. A.; Strzhemechny, Y.; Nguyen, D. *Phys. Rev. Lett.* **1998**, *81*, 3876–3879.
(5) Vanhoorne, P.; Register, R. A. *Macromolecules* **1996**, *29*, 598–604.
(6) Vyprachticky, D.; Morawetz, H.; Fainzilberg, V. *Macromolecules* **1993**, *26*, 339–343.
(7) Klein, R. J.; Zhang, S.; Dou, S.; Jones, B. H.; Colby, R. H.; Runt, J. *J. Chem. Phys.* **2006**, *124*, 144903.
(8) Zhang, S.; Dou, S.; Colby, R. H.; Runt, J. *J. Non-Cryst. Solids* **2005**, *351*, 2825–2830.
(9) Kutsumizu, S.; Goto, M.; Yano, S.; Schlick, S. *Macromolecules* **2002**, *35*, 6298–6305.
(10) Laurer, J.; Winey, K. *Macromolecules* **1998**, *31*, 9106–9108.
(11) Benetatos, N. M.; Smith, B. W.; Heiney, P. A.; Winey, K. I. *Macromolecules* **2005**, *38*, 9251–9257.
(12) Benetatos, N. M.; Heiney, P. A.; Winey, K. I. *Macromolecules* **2006**, *39*, 5174–5176.
(13) Benetatos, N. M.; Chan, C. D.; Winey, K. I. *Macromolecules* **2007**, *40*, 1081–1088.
(14) Benetatos, N. M.; Winey, K. I. *J. Polym. Sci., Part B: Polym. Phys.* **2005**, *43*, 3549–3554.
(15) Benetatos, N. M.; Winey, K. I. *Macromolecules* **2007**, *40*, 3223–3228.
(16) Batra, A.; Cohen, C.; Kim, H.; Winey, K. I.; Ando, N.; Gruner, S. M. *Macromolecules* **2006**, *39*, 1630–1638.
(17) Kirkmeyer, B. P.; Taubert, A.; Kim, J. S.; Winey, K. I. *Macromolecules* **2002**, *35*, 2648–2653.
(18) McLean, S. R.; Doyle, M.; Sauer, B. B. *Macromolecules* **2000**, *33*, 6541–6550.
(19) Sauer, B. B.; McLean, S. R. *Macromolecules* **2000**, *33*, 7939–7949.
(20) Composto, R. J.; Walters, R. M.; Genzer, J. *Mater. Sci. Rep.* **2002**, *38*, 107–180.
(21) Doolittle, R. L. *Nucl. Instrum. Meth. B* **1985**, *9*, 344–351.
(22) Tanaka, P. L.; Oldfield, S.; Neece, J. D.; Mullins, C. B.; Allen, D. T. *Environ. Sci. Technol.* **2000**, *34*, 4470–4473.
(23) Wingenter, O.; Sive, B.; Blake, N.; Blake, D.; Rowland, F. *J. Geophysical Res.* **2005**, *110*, D20308.
(24) Chang, S.; Allen, D. T. *Atmos. Environ.* **2006**, *40*, 512–523.
(25) Jones, R. A.; Kramer, E. *J. Philos. Mag. B* **1990**, *62*, 129.
(26) Walters, R. *Counterion Surface Segregation in Ionomer*. Doctoral Thesis, University of Pennsylvania: Philadelphia, PA, 2003.
(27) Doughery, D. A. *Science* **1996**, *271*, 163–168.
(28) Sunner, J.; Nishizawa, K.; Kebarle, P. *J. Phys. Chem.* **1981**, *85*, 1814–1820.
(29) Fujimura, M.; Hashimoto, T.; Kawai, H. *Macromolecules* **1982**, *15*, 136–144.
(30) Yarusso, D. J.; Cooper, S. L. *Macromolecules* **1983**, *16*, 1871–1880.
(31) Gebel, G.; Lambard, J. *Macromolecules* **1997**, *30*, 7914–7920.
(32) Leibler, L.; Rubinstein, M.; Colby, R. H. *Macromolecules* **1991**, *24*, 4701–4712.
(33) Handlin, D. L.; MacKnight, W. J.; Thomas, E. L. *Macromolecules* **1981**, *14*, 795–801.

MA801756G